Optimization of Nuclear-Renewable Hybrid Energy System Operation in Forward Electricity Market

Jubeyer Rahman, *Student Member, IEEE*, and Jie Zhang, *Senior Member, IEEE*
The University of Texas at Dallas
Richardson, TX 75080 USA
{Jubeyer.Rahman, jiezhang}@utdallas.edu

***Abstract*—In this paper, the optimal operation strategy of a nuclear-renewable hybrid energy system (N-R HES) is explored in a day-ahead market. A grid-connected N-R HES is simulated in a customized day-ahead electricity market simulator to explore the capabilities and benefits of N-R HES by providing both energy and different reserve products. The forward market (i.e., day-ahead) clearing price signal is determined from the market model simulation. Three N-R HES optimization and control strategies are formulated and compared in terms of solution quality and computational efficiency, including: (i) an integrated net export maximization model, (ii) a sequential optimization model, and (iii) a multi-objective optimization model with augmented ϵ-constraint. Results on the modified NREL 118-bus test system show that: (i) N-R HES is able to provide regulation and spinning reserves, and (ii) the optimization that maximizes the reserve export from N-R HES produces the most revenue for N-R HES.**

***Index Terms*—hybrid energy system, forward market, net export, reserve, market clearing price**

NOMENCLATURE

Sets

B	Set of all buses
B_L	Set of load buses
B_{HES}	Set of HES buses
G	Set of generators
G_{HES}	Set of HES generators
L	Set of transmission lines
RS	Set of reserve types
T	Set of time slots

Constants

ΔP_g^k	Generation block size of unit g in block k
C_g^k	Generation cost of unit g in block k
$D_{b,t}$	Load at bus b at the t^{th} interval
DT_g	Minimum down time of unit g
IDT_g	Initial minimum down time of unit g
$IF_{b,g}$	Injection factor of unit g at bus b
IUT_g	Initial minimum up time of unit g
K_g	Number of blocks in generation cost functions of unit g
$Limit_l$	Power flow limit at line l
NL_g	No-load cost of unit g
P_g^{max}	Maximum output of unit g
P_g^{min}	Minimum output of unit g
$PTDF_{l,b}$	Power transfer distribution factor from bus b to line l
R_g^D	Ramp-down limit for unit g
R_g^U	Ramp-up limit for unit g
R_g^{SD}	Ramp-down limit for unit g at shutdown
R_g^{SU}	Ramp-up limit for unit g at start-up
$RC_{g,r}$	Reserve cost of unit g for type r
$RP_{t,r}$	Reserve price at the t^{th} interval for type r
$RRR_{t,r}$	System reserve requirement of type r at time t
SD_g	Shutdown cost of unit g
SU_g	Start-up cost of unit g
UD	Duration of the shutdown process
UD	Duration of the start-up process
UT_g	Minimum up time of unit g
$VOIR_r$	Cost of insufficient reserve of type r

Variables

$\delta_{b,t}$	Load shedding quantity of bus b at the t^{th} interval
$\overline{p}_{g,t}$	Maximum available power output of unit g at the t^{th} interval
$ir_{t,r}$	System level insufficient reserve quantity of type r at the t^{th} interval
$lf_{l,t}$	Line flow at line l at the t^{th} interval
ls_t	Load-shedding penalty at the t^{th} interval
$net_{t,r}^{rr}$	Net reserve export of type r from HES at the t^{th} interval
net_t^p	Net power export from HES at the t^{th} interval
$p^{b,g,t}$	Power output of unit g at bus b at the t^{th} interval
$p_{b,t}^{net}$	Net power injection at bus b at the t^{th} interval
$p_{g,i}^D$	Power output of unit g at the t^{th} interval during shutdown
$p_{g,i}^U$	Power output of unit g at the t^{th} interval during start-up
$p_{g,t}$	Power output of unit g at the t^{th} interval
$p_{g,t}^k$	Power output of unit g at the t^{th} interval in block k
$pc_{g,t}$	Production cost of unit g at the t^{th} interval
$rc_{g,t,r}$	Reserve cost of unit g of type r at the t^{th} interval
$rr_{g,t,reg}$	Regulating reserve from unit g at the t^{th} interval
$rr_{g,t,r}$	Reserve of type r from unit g at the t^{th} interval
$sd_{g,t}$	Shutdown cost of unit g at the t^{th} interval
$su_{g,t}$	Start-up cost of unit g at the t^{th} interval
$v_{g,t}$	Commitment status of unit g at the t^{th} interval

$y_{g,t}$ Starting-up status of unit g at the beginning of the t^{th} interval

$z_{g,t}$ Shutting-down status of unit g at the beginning of the t^{th} interval

I. Introduction

With the advent of more flexible reactors, the synergy of nuclear and renewable resources appears to be a promising solution in energy markets, due to their appealing clean and non-carbon-emitting traits with much less operational costs compared to their counterparts. The benefit of this integrated energy system can be maximized by coupling them together often termed as a nuclear-renewable hybrid energy system (N-R HES). Historically, nuclear plants have been used mainly to serve base load. Beyond classic energy-shifting services, N-R HES may be able to provide a suite of services at finer time-scales to promote a safer and more reliable integration of renewable energy resources. Operating reserves are typically used by grid operators to reduce imbalances due to uncertainties associated with variable load and renewable energy resources and to protect against contingency events. N-R HES may be able to provide a range of ancillary services at multiple time-scales, such as flexible ramping reserves, regulation reserves, and frequency response while capitalizing the potential of its existing components [1].

Three types of N-R HES have been studied in the literature [2]: tightly coupled, thermally coupled, and loosely coupled N-R HES. Tightly coupled N-R HESs are co-located, directly integrated, and co-controlled behind the grid. Thermally coupled N-R HESs have an integrated thermal connection and are co-controlled, but many have multiple electrical connections to the grid and subsystems and may not be co-located. Loosely coupled (or electricity-only) N-R HESs only have electrical interfaces and subsystems that can be located separately with multiple connections to the grid, but they are co-controlled, so a single management entity dispatches the energy and services to the grid. This study focuses on the optimal operation of a tightly coupled N-R HES.

The traditional role of nuclear plants as base-load units is transformed to (i) help tackle the volatility of the increasing penetration of renewable sources, and (ii) explore additional benefits from nuclear plants by providing different energy and power products. In some countries such as France and Germany, system operators have already started to use nuclear plants in load-following regulation services [3]. Studies [4] have shown potential benefits and versatility of N-R HES to the grid, while earning additional revenues through participating into the ancillary service market. Though the viability of grid connected N-R HES makes it more preferable than its standalone counterpart [5], its interaction with the rest of the grid in different market settings remains mostly unexplored. A previous study [6] has explored the impact of N-R HES on forward (day-ahead) market and spot (real-time) market, by assuming that the forward and spot market prices are given and pre-determined.

The current work performs a holistic N-R HES study in a forward market setting by determining the forward market price simultaneously, where N-R HES can participate in both energy and different reserve markets. Instead of using a given price signal, the locational marginal price (LMP) is determined based on the interaction between N-R HES and the rest of the grid. In this study, a day-ahead unit commitment (DAUC) model has been developed to maximize the economic value of grid-connected N-R HES. A tighter control has been imposed on the N-R HES to interact with the grid, based on optimal energy transfer management. The model development has been performed on the basis of the multi-timescale market models of Flexible Energy Scheduling Tool for Integrating Variable Generation (FESTIV) [7]. FESTIV allows for the explicit modeling of reserve deployment and its impacts on system reliability metrics, unlike traditional production cost modeling which only accounts for the holding of reserves.

The rest of the paper is organized as follows. In Section II, optimization methods for DAUC models with N-R HES control are discussed. Section III presents a case study and results of N-R HES operations with different optimization strategies. Section IV concludes the paper.

II. Methodology

To simulate N-R HES in both energy scheduling and ancillary service markets, a production cost minimization model is adopted and modified. While N-R HES can provide a number of reserve products at different timescales, this study only focuses on the day-ahead market model. Three optimization and control strategies are formulated and compared, each focusing on maximizing the operational benefits of N-R HES, including: (i) an integrated net export maximization model, (ii) a sequential optimization model, and (iii) a multi-objective optimization model with augmented ϵ-constraint.

A. Integrated net export maximization model

In this model, the N-R HES operation is given preference over the rest of the grid, with an objective to maximize the net power and reserve export from N-R HES to the power grid. The optimization is performed in an integrated manner, where the N-R HES constraints are incorporated to the system-level constraints. The interaction of N-R HES with the grid is reflected through system-level constraints, such as the bus power balance, total reserve requirement constraints, etc., and the same unit-specific constraints are applied for every component of the N-R HES to be consistent with other grid components. The integrated net export maximization model is formulated as follows.

$$\begin{aligned} \textbf{\textit{min}} \sum_{t\in T}\Bigg[\sum_{g\in G\setminus G_{HES}}(su_{g,t}+sd_{g,t}+pc_{g,t}+\sum_{r\in RS}rc_{g,t,r})+ls_t\Bigg] \\ +\sum_{t\in T}\sum_{r\in RS}VOIR_r ir_{t,r} \\ -\sum_{t\in T}\sum_{g\in G_{HES}}(pc_{g,t}+\sum_{r\in RS}rc_{g,t,r}+su_{g,t}+sd_{g,t}) \end{aligned} \tag{1}$$

s.t.

$$su_{g,t} \geq SU_g[v_{g,t} - v_{g,t-1}], \forall g \in G, \forall t \in T \tag{2}$$

$$sd_{g,t} \geq SD_g[v_{g,t-1} - v_{g,t}], \forall g \in G, \forall t \in T \tag{3}$$

$$pc_{g,t} = NL_g v_{g,t} + \sum_{k=1}^{K_g} p_{g,t}^k C_g^k, \forall g \in G, \forall t \in T \tag{4}$$

$$rc_{g,t,r} = \sum_{g \in G} rr_{g,t,r} RC_{g,r}, \forall g \in G, \forall t \in T, \forall r \in RS \tag{5}$$

$$P_g^{min} v_{g,t} \leq p_{g,t} \leq \overline{p}_{g,t}, \forall g \in G, \forall t \in T \tag{6}$$

$$0 \leq \overline{p}_{g,t} \leq P_g^{max} v_{g,t}, \forall g \in G, \forall t \in T \tag{7}$$

$$\overline{p}_{g,t} - \sum_{r \in RS} rr_{g,t,r} \leq p_{g,t-1} + R_g^U v_{g,t-1} + R_g^{SU}[v_{g,t} - v_{g,t-1}] + P_g^{max}(1 - v_{g,t}), \forall g \in G, \forall t \in T, \forall r \in RS \tag{8}$$

$$\overline{p}_{g,t} \leq R_g^{SD}[v_{g,t} - v_{g,t+1}] + P_g^{max} v_{g,t+1}, \quad \forall g \in G, \forall t = 1, ..., |T| - 1 \tag{9}$$

$$p_{g,t} + \sum_{r \in RS} rr_{g,t,r} \leq \overline{p}_{g,t}, \forall g \in G, \forall t \in T, \forall r \in RS \tag{10}$$

$$p_{g,t-1} - p_{g,t} \leq R_g^D v_{g,t} + R_g^{SD}(v_{g,t-1} - v_{g,t}) + P_g^{max}(1 - v_{g,t-1}), \forall g \in G, \forall t \in T \tag{11}$$

$$p_{g,t} = P_g^{min} v_{g,t} + \sum_{k=1}^{K_g} p_{g,t}^k, \forall g \in G, \forall t \in T \tag{12}$$

$$0 \leq p_{g,t}^k \leq \Delta P_g^k, \forall g \in G, \forall t \in T \tag{13}$$

$$\sum_{t=1}^{IUT_g} (1 - v_{g,t}) = 0, \forall g \in G \tag{14}$$

$$\sum_{\tau=t}^{t+UT_g-1} v_{g,\tau} \geq UT_g(v_{g,t} - v_{g,t-1}), \quad \forall g \in G, \forall t = IUT_g + 1, ..., |T| - UT_g + 1 \tag{15}$$

$$\sum_{\tau=t}^{T} [v_{g,\tau} - (v_{g,t} - v_{g,t-1})] \geq 0, \quad \forall g \in G, \forall t = |T| - UT_g + 2, ..., |T| \tag{16}$$

$$\sum_{t=1}^{IDT_g} v_{g,t} = 0, \forall g \in G \tag{17}$$

$$\sum_{\tau=t}^{t+DT_g-1} (1 - v_{g,t}) \geq DT_g(v_{g,t-1} - v_{g,t}), \quad \forall g \in G, \forall t = IDT_g + 1, ..., |T| - DT_g + 1 \tag{18}$$

$$\sum_{\tau=t}^{T} [1 - v_{g,\tau} - (v_{g,t-1} - v_{g,t})] \geq 0, \quad \forall g \in G, \forall t = |T| - DT_g + 2, ..., |T| \tag{19}$$

$$p_{g,t} \geq P_g^{min} \left[v_{g,t} - \sum_{i=1}^{DD} z_{g,t+i} - \sum_{i=1}^{UD} y_{g,t-i+1} \right] + \sum_{i=1}^{UD} p_{g,i}^U y_{g,t-i+1}, \forall g \in G, \forall t \in T \tag{20}$$

$$p_{g,t} \geq P_g^{min} \left[v_{g,t} - \sum_{i=1}^{DD} z_{g,t+i} - \sum_{i=1}^{UD} y_{g,t-i+1} \right] + \sum_{i=1}^{DD} p_{g,i}^D z_{g,t+DD-i+1}, \forall g \in G, \forall t \in T \tag{21}$$

$$p_{g,t} \leq P_g^{min} \left[v_{g,t} - \sum_{i=1}^{UD} y_{g,t-i+1} \right] + \sum_{i=1}^{UD} p_{g,i}^U y_{g,t-i+1}, \forall g \in G, \forall t \in T \tag{22}$$

$$p_{g,t} \leq P_g^{min} \left[v_{g,t} - \sum_{i=1}^{DD} z_{g,t+i} \right] + \sum_{i=1}^{DD} p_{g,i}^D z_{g,t+DD-i+1}, \forall g \in G, \forall t \in T \tag{23}$$

$$p_{g,t} - p_{g,t-1} \leq P_g^{min} \sum_{i=1}^{UD} y_{g,t-i+1} + R_g^U \left[v_{g,t} - \sum_{i=1}^{UD} y_{g,t-i+1} \right], \forall g \in G, \forall t \in T \tag{24}$$

$$p_{g,t-1} - p_{g,t} \leq P_g^{min} \sum_{i=1}^{DD} z_{g,t+i-1} + R_g^D \left[v_{g,t-1} - \sum_{i=1}^{DD} z_{g,t+i-1} \right], \forall g \in G, \forall t \in T \tag{25}$$

$$y_{g,t} - z_{g,t} = v_{g,t} - v_{g,t-1}, \forall g \in G, \forall t \in T \tag{26}$$

$$v_{g,t} \geq \sum_{i=1}^{UD} y_{g,t-i+1}, \forall g \in G, \forall t \in T \tag{27}$$

$$v_{g,t} \geq \sum_{i=1}^{DD} z_{g,t+i}, \forall g \in G, \forall t \in T \tag{28}$$

$$y_{g,t} + \sum_{i=1}^{UD+DD-1} z_{g,t+i-1} \leq 1, \forall g \in G, \forall t \in T \tag{29}$$

$$p_{g,t} \geq p_{g,UD}^U \left[\sum_{i=1}^{DD} z_{g,t+i} + \sum_{i=1}^{UD} y_{g,t-i+1} - 1 \right], \quad \forall g \in G, \forall t \in T \tag{30}$$

$$p_{g,t} \geq p_{g,1}^D \left[\sum_{i=1}^{DD} z_{g,t+i} + \sum_{i=1}^{UD} y_{g,t-i+1} - 1 \right], \quad \forall g \in G, \forall t \in T \tag{31}$$

$$\sum_{g\in G} p_{g,t} - \sum_{b\in B_L} D_{b,t} - \delta_{b,t} = 0, \forall t \in T \tag{32}$$

$$p^{net}_{b,t} = \sum_{g\in G\setminus G_{HES}} p_{b,g,t} IF_{b,g} - D_{b,t} + \delta_{b,t} + \begin{cases} \sum_{g\in G_{HES}} p_{b,g,t}, & \forall b \in B_{HES}, \forall t \in T \\ 0, & \text{otherwise} \end{cases} \tag{33}$$

$$\delta_{b,t} \leq D_{b,t}, \forall b \in B_L, \forall t \in T \tag{34}$$

$$\sum_{g\in G} rr_{g,t,r} + ir_{t,r} \geq RRR_{t,r}, \forall t \in T, \forall r \in RS \tag{35}$$

$$rr_{g,t,reg} \leq R^{U|D}_g, \forall g \in G, \forall t \in T \tag{36}$$

$$lf_{l,t} = \sum_{b\in B} PTDF_{l,b} p^{net}_{b,t}, \forall l \in L, \forall t \in T \tag{37}$$

$$-Limit_l \leq lf_{l,t} \leq Limit_l, \forall l \in L, \forall t \in T \tag{38}$$

As shown in Eq. 1, the aggregated objective is to minimize the generation cost and load shedding cost of the grid (represented by the first term), while maximizing the generation and reserve cost of the N-R HES (represented by the third term). Unlike the usual unit commitment model formulation, this deduction of N-R HES cost enforces the maximum utilization of N-R HES in both dispatch and the ancillary service market.

Eqs. 2 and 3 define the start-up and shut-down costs, respectively. Eq. 4 represents the cost of production while considering the no-load costs, and Eq. 5 defines the reserve cost. Eqs. 6 and 7 limit the power output of a unit in a particular period by the minimum power output and the maximum available power output (this is also constrained by the unit capacity), respectively. For renewable sources, the maximum available power output can be interpreted as the power forecast. Eqs. 8 through 11 enforce the satisfaction of reserve requirement and ramping capability. Eqs. 12 and 13 implement the aggregated temporal output limit across all the generation cost blocks. Minimum up-time constraints are defined by Eqs. 14 through 16, and minimum down-time constraints are expressed by Eqs. 17, 18, and 19. Eqs. 20 and 21 represent the lower limits for an unit's start-up and shut-down trajectories, respectively. They also bind the ramp-up and ramp-down limits for the particular period. For both start-up and shut-down processes, the first term on the right hand side becomes ineffective and the second term of both Eqs. 20 and 21 effectively controls the start-up and shut-down power trajectory. Similar to Eqs. 20 and 21, Eqs. 22 and 23 set the maximum limit of the power trajectories for the start-up and shut-down process, respectively. Eq. 24 implements the ramp-up limit for all intervals except the starting up period. Eq. 25 represents the ramp-down limitation to nullify the effect of shutdown, and R^D_g is replaced by the machine capacity.

Eq. 26 denotes the shut-down and start-up status change constraint. Eqs. 27 and 28 ensure the unit being online while starting-up or shutting-down, respectively. The start-up and shut-down overlap period constrain the power output to be at the minimum capacity, which is implemented by Eqs. 29, 30, and 31, which are activated at either the last interval of the start-up or the first interval of shut-down. Eqs. 32 to 38 represent system level constraints. Eq. 32 is the system energy balance constraint and Eq. 33 is the bus-wise net energy constraint. For the integrated net export maximization model, the bus-wise net energy constraint has been modified to accommodate the net export from the N-R HES at the point of common coupling (PCC) bus. Eq. 34 represents the load-shedding limit constraint. Eqs. 35 and 36 represent the reserve constraints. Line flows are calculated by using the Power transfer distribution factor (PTDF) matrix in Eq. 37 and their limits are enforced by Eq. 38.

In this work, three types of reserves have been considered, namely regulation reserves, spinning reserves, and non-spinning reserves. The action hierarchy of those reserves are implemented by the difference in the value of insufficient reserves (VOIR). Renewable sources are only allowed to participate in the regulation reserve due to their volatile nature, and other generators' participation to provide different reserves are determined by their characteristics and operational parameter settings. The assumed VOIRs and their time requirement are summarized in Table I, which represent the default reserve settings in FESTIV [7].

Table I
RESERVE PARAMETERS

Type of the reserve	Required time (minutes)	VOIR ($)
Regulation	5	7,500
Spinning	10	5,000
Non-spinning	10	1,500

B. Sequential optimization model

In the sequential optimization model, a mixed-integer programming (MIP) problem representing the grid (excluding the N-R HES) is solved in the first stage, while keeping the net export power and reserve of N-R HES as design variables. Once the net export power and reserve of N-R HES values are determined by solving the grid MIP problem, they are passed to the second stage where an MIP problem representing N-R HES is solved. The generation cost is minimized in the first stage, where the generation and reserve injection from N-R HES do not incur any cost to allow the system to determine the best possible utilization of N-R HES. To ensure the participation of N-R HES at least in the least extent, the minimum net export is set to be greater or equal to the minimum capacity of the N-R HES components (Eq. 40). So, the modified objective function and surplus binding constraints of the sequential optimization model are formulated as follows (for brevity similar system level and machine constraints which are already described in the net export maximization model section are skipped here).

$$\textbf{\textit{min}} \sum_{t\in T} \Big(\sum_{g\in G\setminus G_{HES}} (su_{g,t} + sd_{g,t} + pc_{g,t} + \sum_{r\in RS} rc_{g,t,r}) + ls_t + \sum_{r\in RS} VOIR_r ir_{t,r} \Big) \tag{39}$$

s.t.

$$\sum_{g\in G_{HES}} P_g^{min} \le net_t^p \le \sum_{g\in G_{HES}} P_g^{max}, \quad \forall g \in G_{HES}, t \in T \tag{40}$$

$$p_{b,t}^{net} = \sum_{g\in G\setminus G_{HES}} p_{b,g,t} IF_{b,g} - D_{b,t} + \delta_{b,t} + \begin{cases} net_t^p, & \forall b \in B_{HES}, \forall t \in T \\ 0, & \text{otherwise} \end{cases} \tag{41}$$

$$\sum_{g\in G\setminus G_{HES}} rr_{g,t,r} + ir_{t,r} + net_{t,r}^{rr} \ge RRR_{t,r}, \forall t \in T, \forall r \in RS \tag{42}$$

Similar to the integrated net export maximization model, the bus power injection is calculated by incorporating the net export from N-R HES, which is defined in Eq. 41. The reserve requirement satisfaction constraint is implemented by Eq. 42, where the provision of insufficient reserve is incorporated to represent realistic system operations.

The single machine constraints will remain the same, but slight modifications are performed in the system level constraints. At the second stage of N-R HES optimization, the cost function and binding constraints are formulated as follows.

$$\textbf{\textit{min}} \quad \sum_{t\in T}\sum_{g\in G_{HES}} (su_{g,t} + sd_{g,t} + pc_{g,t} + \sum_{r\in RS} VOIR_r ir_{t,r} + \sum_{r\in RS} rc_{g,t,r}) \tag{43}$$

s.t.

$$net_t^p = \sum_{g\in G_{HES}} p_{g,t}, \forall g \in G_{HES}, \forall t \in T \tag{44}$$

$$net_{t,r}^{rr} = \sum_{g\in G_{HES}} rr_{g,t,r} + ir_{t,r}, \forall g \in G_{HES}, \forall t \in T, r \in RS \tag{45}$$

At the second stage, the N-R HES operation is optimized with an objective of minimizing the generation cost of the N-R HES components and the VOIR. Eqs. 44 and 45 enforce the equality constraints of power and reserve export to the grid, respectively. The N-R HES is allowed to not satisfy the reserve requirement due to the incorporation of insufficient reserve in Eq. 45. Rather than imposing a hard constraint on the reserve requirement satisfaction, the N-R HES is penalized through the VOIR, resembling the industrial practice of independent system operators (ISO). The goal of the second stage optimization is to determine the commitment and ramping details of individual N-R HES components.

C. Multi-objective optimization with augmented ϵ-constraint

Since there exists a conflict of interest in the operation of N-R HES along with rest of the grid, a trade-off point could be explored to maximize the benefits of both the N-R HES and grid entities. To this end, a multi-objective optimization problem is formulated and solved using the augmented ϵ-constraint method. The overall generation cost inclusive of the production cost from N-R HES is minimized, while the N-R HES net revenue from the reserve product is maximized.

$$\textbf{\textit{min}} \sum_{t\in T}\left[\sum_{g\in G}(su_{g,t} + sd_{g,t} + pc_{g,t}) + \sum_{g\in G\setminus G_{HES}}\sum_{r\in RS} rc_{g,t,r}\right] + \sum_{t\in T}(\sum_{r\in RS} VOIR_r ir_{t,r} + ls_t) \tag{46}$$

$$\textbf{\textit{max}} \quad \sum_{t\in T}\left[\sum_{g\in G_{HES}}\left(\sum_{r\in RS} rr_{g,t,r} RP_{t,r}\right)\right] \tag{47}$$

The machine and system level constraints formulations are similar with those in the integrated net export maximization model. The reserve price is collected from the data repository of Electric Reliability Council of Texas (ERCOT) [8]. The reason for choosing the ϵ-constraint method lies in the fact that, it can generate the Pareto frontier for a multi-objective problem. This ϵ-constraint method optimizes one of the objective functions while using the remaining objective functions as constraints. The method consists of the following two phases [9].

- Phase 1: Create a payoff table from the solutions of individual optimization of each objective function;
- Phase 2: Use the payoff table to apply the method for decision-making.

The augmented ϵ-constraint uses lexicographic optimization in the construction of the payoff table (in order to secure the Pareto optimality of individual optima), and a slightly modified objective function to ensure the production of Pareto optimal solutions. The approach ensures that only strongly efficient solutions are filtered out from alternative optimal points.

III. Case Study

A. Experimental setup

In this study, the NREL-118 bus system [10] has been adopted and modified as a test case due to its high penetration of renewable generation. There are 17 wind farms (4.38% installed capacity share) and 75 PV plants (14% installed capacity share) in the system. An N-R HES has been added to the NREL-118 bus system and the N-R HES location is determined empirically. Different component ratings of N-R HES have been compared at different buses with high load shares, and the whole system is simulated in the day-ahead unit commitment environment for a 24-hour period of January 1st, 2024.

By comparing all the locations, bus-82 is selected for N-R HES installation, due to the least operational cost and the highest accommodation capability. Since the DAUC model simulation requires renewable power and load forecasts, the default day-ahead forecasts from the NREL 118-bus system

repository are used [11]. While the forecasting accuracy of renewable generation and load might significantly impact the simulation results (e.g., N-R HES generation, reserve schedules, commitment status, etc.) [12], [13], this paper focuses on the N-R HES modeling and optimization formulation, and the impacts of renewable/load forecasts will be explored in the future. Reserve requirements are determined by following the default FESTIV reserve rule [7] where the regulation reserve varies with the system load and other reserves are set at fixed values.

The specifications of the N-R HES components like nuclear plants are chosen from publicly available sources and the literature [14], [15]. In this study, the N-R HES consists of the following components:

- A nuclear plant of 450 MW capacity.
- A wind plant of 149.5 MW capacity.

B. Results & discussion

Since this study focuses on the day-ahead market, the hourly scheduling results for both generation and reserves of the N-R HES are compared for all three optimization models. Forward market signals are also generated and compared.

Figure 1 compares the N-R HES net power export schedule. Since both the net export maximization and sequential optimization model focus on maximizing the scheduled power export at a minimum cost, a significantly higher amount of energy export from N-R HES is observed compared to that resulted from the augmented ϵ-constraint method. The focus of the augmented ϵ-constraint method is to maximize the revenue from the reserve export, and thus the reserve export from N-R HES is comparatively higher than that from the other two methods. Figures 2 and 3 show the net regulation and spinning reserve schedules of N-R HES, respectively. In terms of regulation reserve, the augmented ϵ-constraint approach enforces a higher participation from the N-R HES, due to the higher reserve price and VOIR. In terms of spinning reserve, the N-R HES shows more participation with the sequential optimization approach compared to the other two approaches. The N-R HES does not participate in the non-spinning reserve market in neither of the optimization approaches, since none of its generating components is offline during the whole simulation horizon.

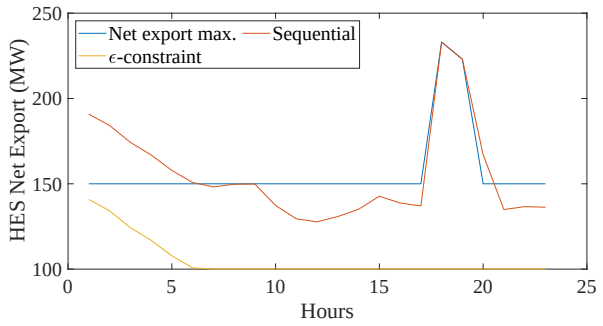

Figure 1. Comparison of the three optimization models: N-R HES net power export schedule to the grid.

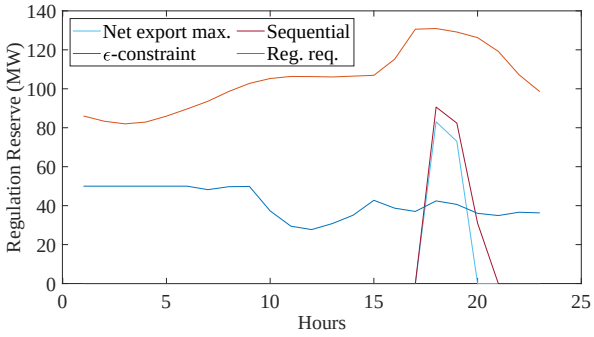

Figure 2. Comparison of the three optimization models: regulating reserve schedule of the N-R HES and the total system regulation reserve requirement.

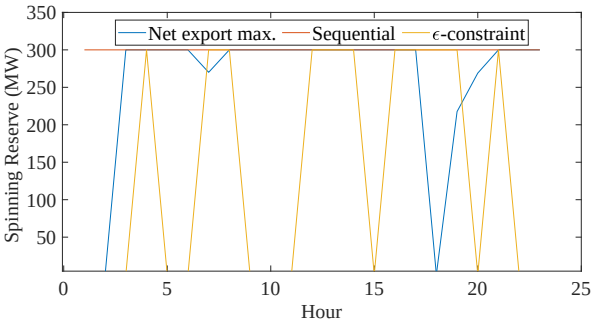

Figure 3. Comparison of the three optimization models: spinning reserve schedule of the N-R HES (the total spinning reserve requirement is 940 MW).

The N-R HES bus price signals (i.e., LMP) from these three optimization models are compared in Fig. 4. By comparing the three LMP profiles, it is observed that LMPs generated from the net export maximization model and the sequential optimization model are higher than that from the augmented ϵ-constraint method. The higher LMPs of the net export maximization model and the sequential optimization model are partially due to the higher energy export of N-R HES. The higher power injection from N-R HES to the grid could potentially cause line congestion (i.e., it causes some of the corresponding variables to their limit and affects the shadow price), and thus impact the LMP. The high LMPs occur at around peak hours when many of the system components are operating at their limits.

To evaluate the efficiency of the three optimization approaches, Table II compares the total production cost, revenue earned from the reserve export, and computational time. For the net export maximization model, the power production cost of N-R HES is added back to the production cost of the rest of the system after the simulation is completed. Similarly, for the sequential optimization model, the production cost in stage-2 is added to the cost incurred in the first stage. The augmented ϵ-constraint method yields the most reserve revenue for the N-R HES, whereas the other two methods produce similar amount of revenue. In terms of computational efficiency, the net export maximization model performs the best, followed

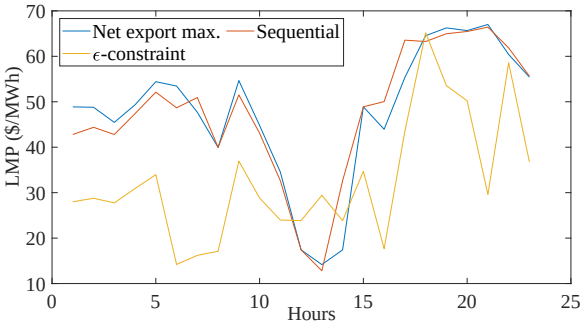

Figure 4. Comparison of the N-R HES bus LMPs from three optimization models.

by the sequential optimization model, and the augmented ϵ-constraint method is significantly slower. All the simulations were performed on a high performance computing facility (Ganymede [16]) using 40 processors and 64-GB memory.

Table II
COMPARISON OF PRODUCTION COST, RESERVE REVENUE, AND SOLUTION TIME

Optimization model	Total production cost ($)	HES reserve revenue ($)	Solution time (s)
Net export max.	237,906,757.45	3,982.9	20.39
Sequential	236,446,206.95	4,051.2	48.43
ϵ-constraint	235,367,623.37	8,203.5	24,109

IV. CONCLUSION

This study developed a nuclear-renewable hybrid energy system (N-R HES) operation framework to provide different types of grid products. The capabilities and benefits of N-R HES to provide both energy and reserve products were simulated and explored. Specifically, three N-R HES optimization and control strategies were developed and compared to maximize the economic benefits of N-R HES from a system level perspective. The integrated net export maximization model maximized both the power and reserve export to the grid at a minimum cost; the sequential optimization model ensured the best possible utilization of N-R HES via a two-stage optimization process; the ϵ-constrained method enforced the maximum possible participation of N-R HES in a forward ancillary service market.

Results on a modified NREL-118 bus system have shown that N-R HES is able to support the grid by providing both energy and regulation reserve, thereby increasing the economic efficiency of N-R HES and the reliability of the power grid (the calculated CPS2 value (97.4%) is beyond the required threshold set for systems with similar load profile). So, the N-R HES can earn revenue not only from its energy products but also from its ancillary services. Potential future work will investigate the N-R HES operation on finer timescales, and study the impact of N-R HES on spot market setting while addressing the stochastic characteristics of its renewable components under different realistic scenarios [17].

ACKNOWLEDGMENT

This material is based upon work supported by the the U.S. Department of Energy under Award No. DE-NE0008899.

REFERENCES

[1] M. Cui, J. Zhang, H. Wu, and B.-M. Hodge, "Wind-friendly flexible ramping product design in multi-timescale power system operations," *IEEE Transactions on Sustainable Energy*, vol. 8, no. 3, pp. 1064–1075, 2017.

[2] C. McMillan, R. Boardman, M. McKellar, P. Sabharwall, M. Ruth, and S. Bragg-Sitton, "Generation and use of thermal energy in the us industrial sector and opportunities to reduce its carbon emissions," tech. rep., National Renewable Energy Lab.(NREL), Golden, CO (United States), 2016.

[3] Y. Xu, Z. Wang, W. Sun, S. Chen, Y. Wu, and B. Zhao, "Unit commitment model considering nuclear power plant load following," in *2011 International Conference on Advanced Power System Automation and Protection*, vol. 3, pp. 1828–1832, IEEE, 2011.

[4] H. E. Garcia, J. Chen, J. S. Kim, M. G. McKellar, W. R. Deason, R. B. Vilim, S. M. Bragg-Sitton, and R. D. Boardman, "Nuclear hybrid energy systems regional studies: West texas & northeastern arizona," tech. rep., Idaho National Lab.(INL), Idaho Falls, ID (United States), 2015.

[5] B. E. Türkay and A. Y. Telli, "Economic analysis of standalone and grid connected hybrid energy systems," *Renewable energy*, vol. 36, no. 7, pp. 1931–1943, 2011.

[6] J. Chen and H. E. Garcia, "Economic optimization of operations for hybrid energy systems under variable markets," *Applied energy*, vol. 177, pp. 11–24, 2016.

[7] E. Ela, B. Palmintier, I. Krad, *et al.*, "FESTIV (Flexible energy scheduling tool for integrating variable generation)," tech. rep., National Renewable Energy Lab.(NREL), Golden, CO (United States), 2019.

[8] ERCOT, "Real-time market." [Online] Available at: http://www.ercot.com/mktinfo/rtm. [Accessed: 10 Nov. 2020].

[9] G. Mavrotas and K. Florios, "Augmecon2: A novel version of the ε-constraint method for finding the exact pareto set in multi-objective integer programming problems," *Applied Mathematics and Computation*, vol. 219, no. 18, pp. 9652–9669, 2013.

[10] I. Pena, C. B. Martinez-Anido, and B.-M. Hodge, "An extended ieee 118-bus test system with high renewable penetration," *IEEE Transactions on Power Systems*, vol. 33, no. 1, pp. 281–289, 2017.

[11] NREL, "NREL-118 system database." [Online] Available at: http://www.nrel.gov/esif/assets/docs/input-files.zip. [Accessed: 10 Nov. 2020].

[12] M. Cui, J. Zhang, B.-M. Hodge, S. Lu, and H. F. Hamann, "A methodology for quantifying reliability benefits from improved solar power forecasting in multi-timescale power system operations," *IEEE Transactions on Smart Grid*, vol. 9, no. 6, pp. 6897–6908, 2017.

[13] B. Li and J. Zhang, "A review on the integration of probabilistic solar forecasting in power systems," *Solar Energy*, vol. 207, pp. 777–795, 2020.

[14] TAMU, "Electric grid test case repository." [Online] Available at: https://electricgrids.engr.tamu.edu/electric-grid-test-cases/activsg2000/. [Accessed: 10 Nov. 2020].

[15] A. Lokhov, "Load-following with nuclear power plants," *NEA news*, vol. 29, no. 2, pp. 18–20, 2011.

[16] "Ganymede-user-guide." [Online] Available at: http://docs.oithpc.utdallas.edu/. [Accessed: 2 March, 2020].

[17] B. Li, K. Sedzro, X. Fang, B.-M. Hodge, and J. Zhang, "A clustering-based scenario generation framework for power market simulation with wind integration," *Journal of Renewable and Sustainable Energy*, vol. 12, no. 3, p. 036301, 2020.